RON receptor tyrosine kinase regulates glycolysis through MAPK/CREB signaling to affect ferroptosis and chemotherapy sensitivity of thyroid cancer cells

XIN JIN*, HAONAN ZHU*, XINGYU CHEN, YINING YANG and DONGLIANG SONG

School of Medicine, Shaoxing University, Shaoxing, Zhejiang 312000, P.R. China

Received January 11, 2024; Accepted June 14, 2024

DOI: 10.3892/mmr.2024.13359

Abstract. Anaplastic thyroid cancer (ATC) is one of the deadliest and most aggressive human malignancies for which there is currently no effective treatment. Tyrosine kinase receptor RON is highly expressed in various cancer types, including colon, pancreatic and thyroid cancer. However, its underlying role in ATC is not fully understood. The present study investigated the therapeutic potential and molecular mechanism of RON in ATC. RON expression in thyroid cancer cells was detected by western blotting. Glycolysis was assessed by measuring the extracellular acidification rate, glucose uptake, lactate concentration, and expression levels of glucose transporter 1, hexokinase 2 and pyruvate kinase M1/2. In addition, ferroptosis was assessed by detecting the levels of total iron, lipid peroxide and reactive oxygen species, and the expression levels of ferroptosis-related proteins. Furthermore, mitochondrial function were assessed by JC-1 staining and detection kits, respectively. The results demonstrated that RON was highly expressed in thyroid cancer cell lines. Furthermore, RON interference inhibited glycolysis, promoted ferroptosis, elevated cell sensitivity to chemotherapy and affected mitochondrial function in thyroid cancer cells. Further experiments demonstrated that RON interference affected the ferroptosis levels in thyroid cancer cells by inhibiting the glycolysis process. Mechanistically, the present results indicated that RON may affect ferroptosis, glycolysis and chemotherapy sensitivity by regulating MAPK/cAMP-response element binding protein (CREB) signaling in thyroid cancer cells. In conclusion, the present study demonstrated that RON affected ferroptosis, glycolysis and chemotherapy sensitivity in thyroid cancer cells by regulating MAPK/CREB signaling, demonstrating its potential as a therapeutic target in thyroid cancer cells.

Correspondence to: Dr Xin Jin, School of Medicine, Shaoxing University, Nanshan Campus, 900 Chengnan Road, Shaoxing, Zhejiang 312000, P.R. China
E-mail: merry_Jin@outlook.com

*Contributed equally

Key words: anaplastic thyroid cancer, RON, glycolysis, ferroptosis, chemotherapy sensitivity, MAPK/cAMP-response element binding protein

Introduction

Thyroid cancer has the ninth highest cancer incidence worldwide according to the GLOBOCAN 2020 database of cancer incidence and mortality by the WHO International Agency for Research on Cancer (1). Thyroid cancer is traditionally classified as differentiated thyroid cancer or anaplastic thyroid cancer (ATC) based on the degree of differentiation (2). ATC is a rare but aggressive form of thyroid cancer. Although ATC accounts for 2-5% of all thyroid cancers worldwide, half of all thyroid cancer-related deaths are attributed to ATC (3,4). Due to its high proliferation rate and invasive behavior, ATC accounts for 40-50% of most thyroid cancer-related deaths worldwide (5). The median survival time of patients with ATC is 3-5 months, and it is estimated that the 1-year survival rate is between 10 and 20% (6,7). ATC typically shows a limited response to conventional treatments such as radioactive iodine and chemotherapy, leaving limited and largely ineffective treatment options for ATC (8).

In theory, the molecular pathogenesis of ATC involves the dysregulation of multiple signal transduction pathways including TP53, TERT promoter, PI3K/AKT/mTOR pathway effectors, SWI/SNF subunits and histone methyltransferase (9). The abnormal expression of receptor tyrosine kinases (RTKs), which is associated with gene point mutations, amplification and protein upregulation, has been detected in cancer samples including lung, esophageal and thyroid cancers and contributes to diverse malignant behaviors such as gain-of-function mutations, genomic amplification, chromosomal rearrangements and autocrine activation (10). The use of small chemical inhibitors or monoclonal antibodies such as bevacizumab and cetuximab to target RTKs has shown effectiveness in cancer treatment, and thus, comprehending the intricate mechanisms of RTK regulation is of clinical significance (11,12). Tyrosine kinase receptor RON, also termed macrophage stimulating protein receptor, is a typical RTK belonging to the methionine family and serves a role in regulating the malignant behavior of specific cancer types through altered RON expression (13,14). Furthermore, RON-transduced signals are essential components for the proliferation and survival of thyroid cancer cells (15). A recent study demonstrated that RON could enhance cholesterol

biosynthesis, while upregulating the glycolytic enzyme hexokinase 2 (HK2), thereby serving a role in breast cancer (16). In addition, HK2 serves a pivotal role in influencing the ferroptosis process of tumor cells (17). However, it remains unclear whether RON can regulate glycolysis and ferroptosis processes in ATC, and whether the mechanism involved in influencing ferroptosis is linked to glycolysis.

Recent research has indicated that RON can promote the migration and invasion of bladder cancer cells by activating MAPK/ribosomal s6 kinase (RSK)/cAMP-response element binding protein (CREB) signaling (18). Notably, its downstream CREB signaling can affect ferroptosis and reduce myocardial damage, and can also affect the glycolysis process in hepatocellular carcinoma cells (19,20). Additionally, CREB signaling has been reported in breast cancer, but related mechanisms such as glycolysis and ferroptosis have not yet been explored (21). Therefore, the present study aimed to explore RON expression, and its effect on glycolysis, ferroptosis and chemotherapy sensitivity of thyroid cancer cells *in vitro*, and explore its potential mechanisms.

Materials and methods

Cell culture and establishment of doxorubicin (Dox)-resistant ATC cells. The KHM-5M human ATC cell line was purchased from Cellverse Bioscience Technology, Co., Ltd. BHT101, 8305C and ACT-1 cell lines were obtained from The Cell Bank of Type Culture Collection of The Chinese Academy of Sciences. The Nthy-ori 3-1 normal human thyroid cell line was obtained from Cellverse Bioscience Technology Co., Ltd. All cells were cultured in RPMI-1640 medium (Thermo Fisher Scientific, Inc.) containing 10% FBS and 1% penicillin/streptomycin solution at 37˚C in a humidified atmosphere of 5% CO_2. In addition, 8305C cells were treated with the p38 MAPK agonist P79350 (50 μM) for 24 h at 37˚C.

To establish the Dox-resistant ATC cells, cells were selected using stepwise increasing concentrations of Dox (0.01-1 μM). Finally, cells were maintained in 1 μM Dox for the resistance characteristics and referred to as 8305C/Dox cells. At 1 week before the experiment, the medium with Dox was removed and replaced with normal medium (22).

Small interfering RNA (siRNA) transfection. The RON-specific siRNA (si-RON#1: GGAGUACUAUAGUGU UCAACA; si-RON#2: GGAACAAAUGACUAUUAAAGC), the corresponding negative control (si-NC: UUCUCCGAA CGUGUCACGU), the HK2-specific pcDNA overexpression vector (Ov-HK2) and the empty vector (Ov-NC) as a negative control were all provided by Shanghai GeneChem Co., Ltd. Lipofectamine® 3000 (Wuhan Kehaojia Biotechnology Co., Ltd.) was used to transfect the aforementioned recombinants (100 nM) into ATC cells for 48 h at 37˚C according to the recommended instructions. After 48 h transfection, cells were collected for subsequent experiments.

Western blotting. The proteins, which were isolated from ATC cells using RIPA lysis buffer (Bio-Rad Laboratories, Inc.), were quantified using a BCA protein assay kit (Thermo Fisher Scientific, Inc.) according to the standard protocol. After separation by 8% SDS-PAGE, the proteins (30 μg) were transferred onto PVDF membranes. The PVDF membranes were blocked with 5% non-fat milk for 1 h at 25˚C, and incubated overnight at 4˚C with primary antibodies, including anti-glutathione peroxidase 4 (GPX4; cat. no. ab125066; dilution, 1:400; Abcam), anti-ferritin heavy chain 1 (FTH1; cat. no. ab75972; dilution, 1:500; Abcam), anti-solute carrier family 7 member 11 (SLC7A11; cat. no. ab307601; dilution, 1:400; Abcam), anti-acyl-CoA synthetase long chain family member 4 (ACSL4; cat. no. ab155282; dilution, 1:1,500; Abcam), anti-glucose transporter 1 (GLUT1; cat. no. ab115730; dilution, 1:400; Abcam), anti-HK2 (cat. no. ab209847; dilution, 1:1,000; Abcam), anti-pyruvate kinase M1/2 (PKM2; cat. no. ab85555; dilution, 1:1,500; Abcam), Bcl-2 (cat. no. ab32124; dilution, 1:1,000; Abcam), Bax (cat. no. ab32503; dilution, 1:1,000; Abcam), cleaved-caspase3 (cat. no. ab32042; dilution, 1:500; Abcam), caspase3 (cat. no. ab32351; dilution, 1:500; Abcam), ERK (cat. no. ab184699; dilution, 1:1,000; Abcam), p-ERK (cat. no. ab201015; dilution, 1:1,000; Abcam), MAPK (cat. no. ab182453; dilution, 1:1,000; Abcam), p-MAPK (cat. no. ab308038; dilution, 1:1,000; Abcam), CREB (cat. no. ab32515; dilution, 1:1,000; Abcam), p-CREB (cat. no. ab32096; dilution, 1:1,000; Abcam) and β-actin (cat. no. ab8226; dilution, 1:2,500; Abcam) antibodies, followed by incubation with the HRP-labeled secondary anti-rabbit antibody (cat. no. ab109489; dilution, 1:1,000; Abcam) at room temperature for 2 h. The protein bands were visualized using an ECL detection system (Beyotime Institute of Biotechnology). The density of the band was determined using ImageJ software (version 1.49; NIH).

Measurement of the extracellular acidification rate (ECAR). The ECAR was assessed using the Seahorse XFe 96 Extracellular Flux Analyzer (Seahorse Bioscience; Agilent Technologies, Inc.) with the Seahorse XF Glycolysis Stress Test Kit (Seahorse Bioscience; Agilent Technologies, Inc.) according to the manufacturer's protocols. The data were analyzed by the aforementioned analyzer and ECAR detection was noted as mPH/min.

Glucose uptake and lactic acid concentration. The level of glucose uptake in 8305C cells was measured using the Glucose Uptake Assay Kit (Colorimetric; cat. no. ab136955; Abcam). To measure the lactic acid concentration in culture medium from 8305C cells, the lactic acid assay kit (Nanjing Jiancheng Bioengineering Institute) was used according to the manufacturer's instructions.

Ferroptosis analysis. Cells were transfected with si-RON with or without Ov-HK2 and were seeded into 96-well plates. The total iron level was detected by the Iron Assay Kit (ScienCell Research Laboratories, Inc.) in keeping with the recommendation of manufacturer. Finally, the absorbance of the cells was read at 590 nm by means of a spectrophotometer (Shanghai Mapada Instruments, Co., Ltd.).

The reactive oxygen species (ROS) levels of the cells were assessed using 20,70-dichlorofluorescein diacetate (DCFH-DA) staining. In brief, treated cells were collected and washed three times with PBS, then cells were incubated in DCFH-DA (10 mM) at 37˚C for 30 min in darkness. The cells were then washed with PBS three times and the fluorescence

images were obtained by a fluorescence microscope at excitation wavelength of 485 nm and emission wavelength of 520 nm.

Mitochondrial membrane potential assay. The mitochondrial membrane potential was examined using JC-1 (Beyotime Institute of Biotechnology) according to the manufacturer's instructions. Briefly, 8305C cells were cultured in 6-well plates ($3x10^5$ cells per well). After 24 h of growth, cells were treated with superparamagnetic iron oxide-serum at a concentration of 100 μg Fe/ml for 24 h at 37˚C. After staining with JC-1 according to the manufacturer's protocol, the cells were analyzed by fluorescence microscopy (BD Biosciences). Mitochondrial integrity was quantified by measuring the fluorescence intensity of J-aggregates. Green fluorescence represented the monomeric form of JC-1, appearing in the cytosol after mitochondrial membrane depolarization. Red emission of the dye represented a potential-dependent aggregation in the mitochondria, reflecting $\Delta\Psi m$. The excitation wavelength of JC-1 is 488 nm, and the approximate emission wavelength of the monomeric and J-aggregate forms is 529 and 590 nm, respectively.

Intracellular ATP detection assay. The cells were trypsinized and lysed with the lysis buffer provided in the commercial kit on ice. The supernatant of the lysate was collected and incubated with the ENLITEN® ATP assay system (Promega Corporation) according to the manufacturer's protocol. The luminescence was detected using a spectrophotometer (BioTek Synergy H1; Agilent Technologies, Inc.).

Detection of biochemical factors. The levels of reduced glutathione (GSH) in cell lysates were examined using a Glutathione Assay Kit (cat. no. #CS0260; Sigma-Aldrich; Merck KGaA) according to the manufacturer's instructions. The levels of malondialdehyde (MDA) and 4-hydroxynonenal (4-HNE), and the activities of superoxide dismutase (SOD) and GSH peroxidase (GSH-Px) were detected using the MDA assay kit, 4-HNE assay kit, SOD assay kit and GSH-Px assay kit (all Nanjing Jiancheng Bioengineering Institute), respectively, according to the manufacturer's instructions.

Flow cytometry. Apoptosis was detected by flow cytometry with Annexin V/PI double staining. Briefly, 8305C cells and 8305C/Dox cells were washed with PBS and re-suspended in binding buffer. Next, FITC-conjugated anti-annexin-V staining antibody (BD Biosciences) and PI solution were mixed and gently resuspended in Annexin V Binding buffer. Following incubation of cells, flow cytometry was performed using a flow cytometer (Becton, Dickinson and Company). The data were analyzed using FlowJo software (version 10; Tree Star, Inc.).

Statistical analysis. Data are expressed as the mean ± SD of results derived from three independent experiments performed in triplicate. The results were analyzed using GraphPad Prism 8.0 software (Dotmatics). Differences in multiple groups were compared using one-way ANOVA followed by Tukey's post hoc test. $P<0.05$ was considered to indicate a statistically significant difference.

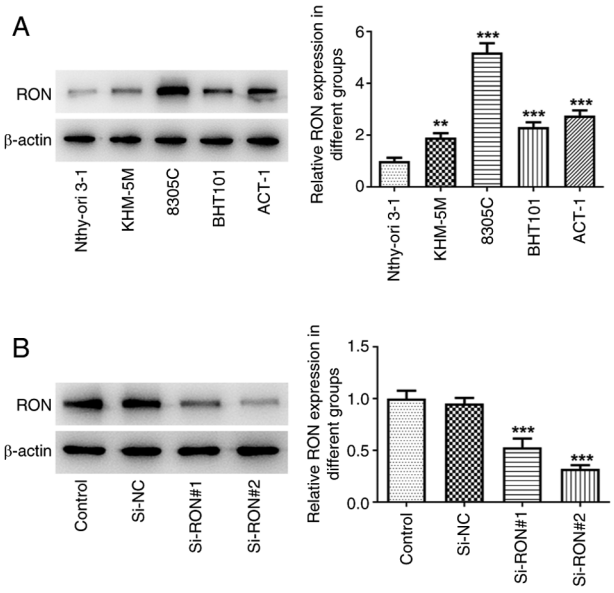

Figure 1. Expression of RON in thyroid cancer cells. (A) Relative RON protein expression in thyroid cancer cells lines (KHM-5M, 8305C, BHT101 and ACT-1) vs. normal human thyroid cells (Nthy-ori-3-1); (B) relative RON protein expression after transfection. $^{**}P<0.01$, $^{***}P<0.001$ vs. si-NC. NC, negative control.

Results

RON is highly expressed in thyroid cancer cells. RON expression in KHM-5M, BHT101, 8305C and ACT-1 thyroid cancer cell lines was examined by western blotting. The results demonstrated that RON expression was higher in thyroid cancer cells compared with in Nthy-ori 3-1 normal human thyroid cells, with the most pronounced increase in 8305C cells (Fig. 1A). Therefore, 8305C cells were selected for the subsequent experiments. Subsequently, in order to further study the mechanism of RON, transfection was used to interfere with RON expression (Fig. 1B). si-RON#2 had a more effective knockdown effect and was thus selected for the following assays (termed si-RON).

RON interference inhibits glycolysis in 8305C cells. The effect of RON interference on glycolysis in 8305C cells was studied. The results demonstrated that the levels of ECAR, lactic acid and glucose in the RON-silenced 8305C cell culture medium were reduced compared with the negative group (Fig. 2A-C). Furthermore, western blotting indicated that the expression levels of HK2 and PKM2 were decreased in the si-RON 8305C cell group compared with the negative group (Fig. 2D). Taken together, these data suggested that RON interference inhibited glycolysis in thyroid cancer cells.

RON interference increases ferroptosis levels in 8305C cells. To investigate the role of ROS in si-RON group-induced ferroptosis, the DCFH-DA probe was used to monitor intracellular ROS production. After RON interference, total iron, intracellular ROS, MDA and 4-HNE levels were markedly increased, and SOD and GSH-Px levels and the levels of the ferroptosis-related proteins GPX4, FTH1 and SLC7A11 were markedly decreased, while the protein expression levels

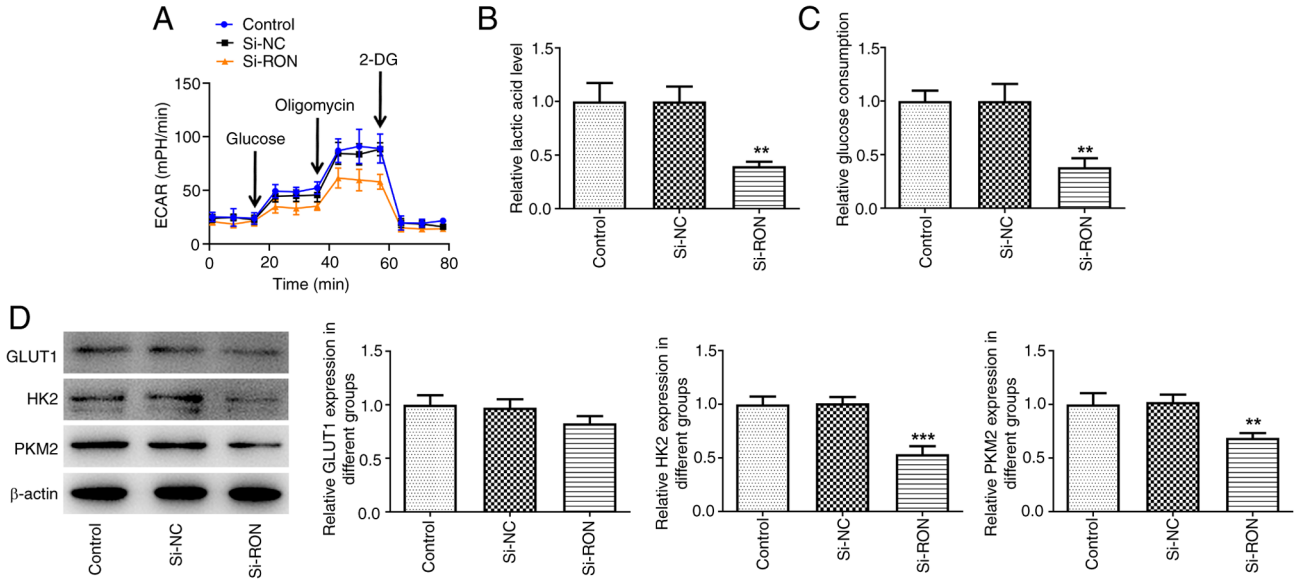

Figure 2. Effects of interference with RON on glycolysis in thyroid cancer cells. (A) ECAR assessment; (B) levels of lactic acid; (C) levels of glucose; (D) protein levels of GLUT1, HK2 and PKM2 were estimated by western blotting. **P<0.01, ***P<0.001 vs. si-NC. ECAR, extracellular acidification rate; HK2, hexokinase 2; GLUT1, glucose transporter 1; PKM2, pyruvate kinase M1/2; NC, negative control.

of ACSL4 were markedly increased in thyroid cancer cells compared with the negative group (Fig. 3A-D). These results suggested that si-RON induced ferroptosis in 8305C cells.

RON interference inhibits Dox resistance in 8305C cells. The results of flow cytometry demonstrated that, compared with that of the corresponding control cells, the apoptosis level of 8305C/Dox cells was markedly increased, and the percentage of apoptotic cells after RON interference was markedly higher compared with the negative group (Fig. 4A and B). To evaluate whether RON interference is involved in the development of Dox resistance in thyroid cancer cells, western blotting was used to evaluate the expression changes of apoptosis-related proteins in the 8305C/Dox cell line following RON interference (Fig. 4C and D). The present data confirmed that RON silencing increased the sensitivity of 8305C/Dox cells to apoptotic cell death, as illustrated by a higher percentage of apoptotic cells, and increased the expression of Bax (pro-apoptotic) and cleaved caspase3, and reduced the Bcl2 level. These results indicated that RON interference was associated with Dox resistance in 8305C cells.

RON interference affects mitochondrial function in 8305C cells. The mitochondrial membrane potential reflects the normal structure and function of mitochondria, while depolarization of the membrane potential suggests that the structure and function of mitochondria are impaired (23). In the present study, the mitochondrial membrane potential in thyroid cancer cells was detected using a JC-1 fluorescence probe. Compared with the si-NC group, si-RON caused the depolarization of the mitochondrial membrane potential in 8305C cells (Fig. 5A). Furthermore, the ATP content was decreased, while the mitochondrial ROS content of thyroid cancer cells was increased after RON interference (Fig. 5B and C).

RON interference affects ferroptosis levels in 8305C cells by inhibiting the glycolysis process. Previous data has shown that RON had a high impact on HK2 (24), so it was hypothesized that RON may affect the glycolysis process through HK2. Therefore, a HK2 overexpression plasmid was constructed to explore its effect of glycolysis on ferroptosis in thyroid cancer cells by regulating the expression of HK2 (Fig. 6A). To further explore the effects of RON on the level of ferroptosis in thyroid cancer cells by inhibiting the glycolytic process, the DCFH-DA probe was used to monitor intracellular ROS production. The results demonstrated that HK2 overexpression reversed the effects of RON interference on total iron, intracellular ROS, MDA, 4-HNE, SOD and GSH-Px levels, as well as the expression levels of ferroptosis-related proteins, including GPX4, FTH1, SLC7A11 and ACSL4 (Fig. 6B-E). These results indicated that RON interference affected the level of ferroptosis in thyroid cancer cells by inhibiting the glycolytic process.

RON interference affects chemotherapy sensitivity of 8305C cells by regulating HK2 in glycolysis. The present study further explored whether RON interference affects chemotherapy sensitivity in thyroid cancer cells by regulating HK2 in glycolysis. The results demonstrated that HK2 overexpression reversed the effects of RON interference on the apoptosis rate of cells, and the expression levels of the apoptosis-related proteins Bax, cleaved caspase3 and Bcl2 (Fig. 7A-D). The results indicated that RON interference affected ferroptosis of 8305C cells by regulating the expression of HK2 in glycolysis of thyroid cancer cells.

RON interference affects mitochondrial function in 8305C cells by regulating HK2 in glycolysis. To further explore the effect of RON interference on the mitochondrial function of thyroid cancer cells via regulation of HK2 in glycolysis, the

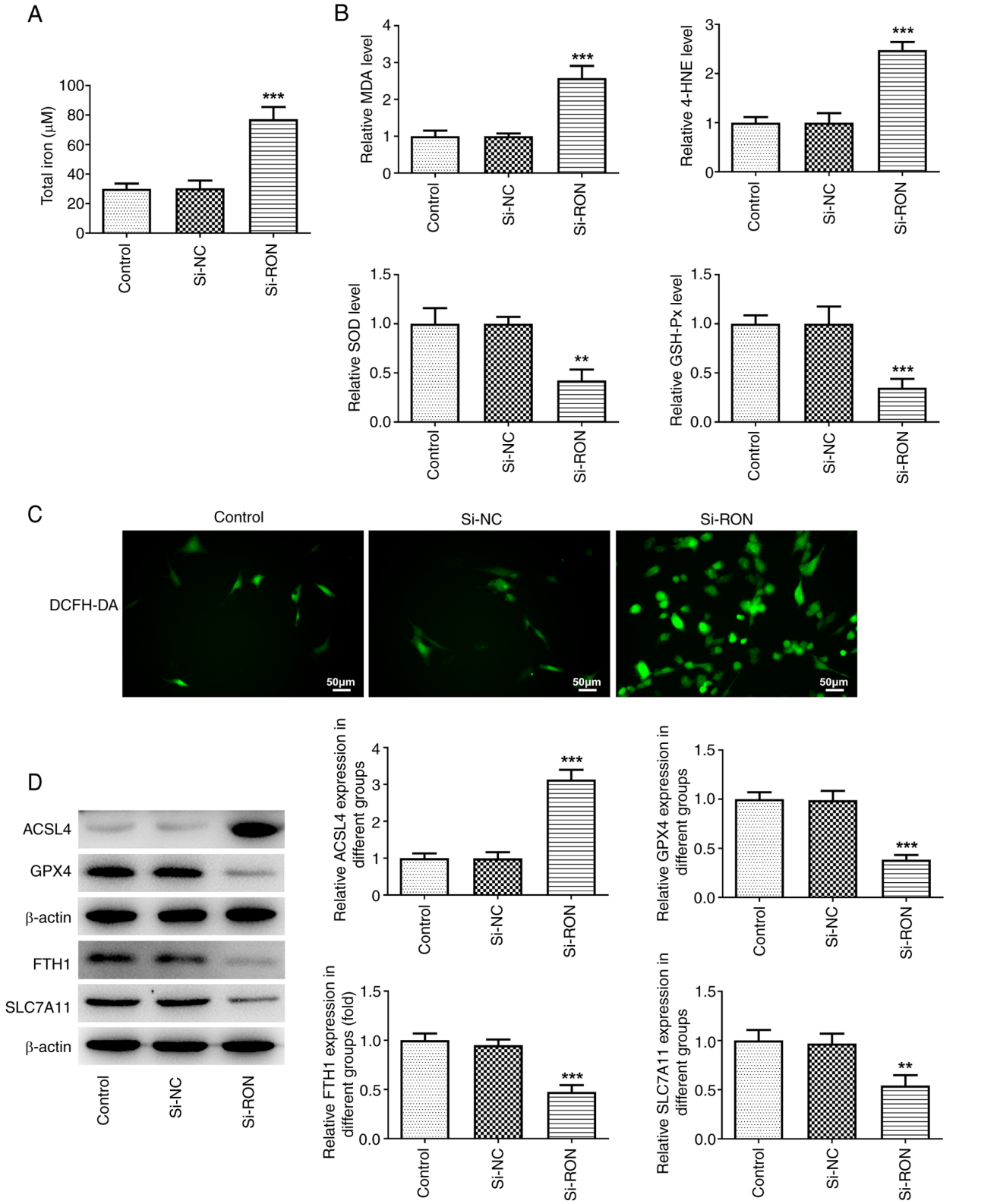

Figure 3. Effects of interference with RON on ferroptosis in thyroid cancer cells. (A) Total iron levels; (B) levels of MDA, 4-HNE, SOD and GSH-Px levels; (C) intracellular ROS levels; (D) protein levels of ferroptosis-related proteins ACSL4, GPX4, FTH1, and SLC7A11 were estimated by western blotting. **P<0.01, ***P<0.001 vs. si-NC. NC, negative control; MDA; malondialdehyde; 4-HNE, 4-hydroxynonenal; SOD, superoxide dismutase; GSH-Px, glutathione peroxidase; ROS, reactive oxygen species; ACSL4, acyl-CoA synthetase long chain family member 4; GPX4, glutathione peroxidase 4; FTH1, ferritin heavy chain 1; SLC7A11, solute carrier family 7 member 11.

JC-1 fluorescent probe was used to detect the mitochondrial membrane potential, and then the levels of ATP and ROS were detected. The results suggested that HK2 overexpression reversed the effects of RON interference on the depolarization of the mitochondrial membrane potential, mitochondrial ROS and ATP content (Fig. 8A-C). Thus, RON interference affected

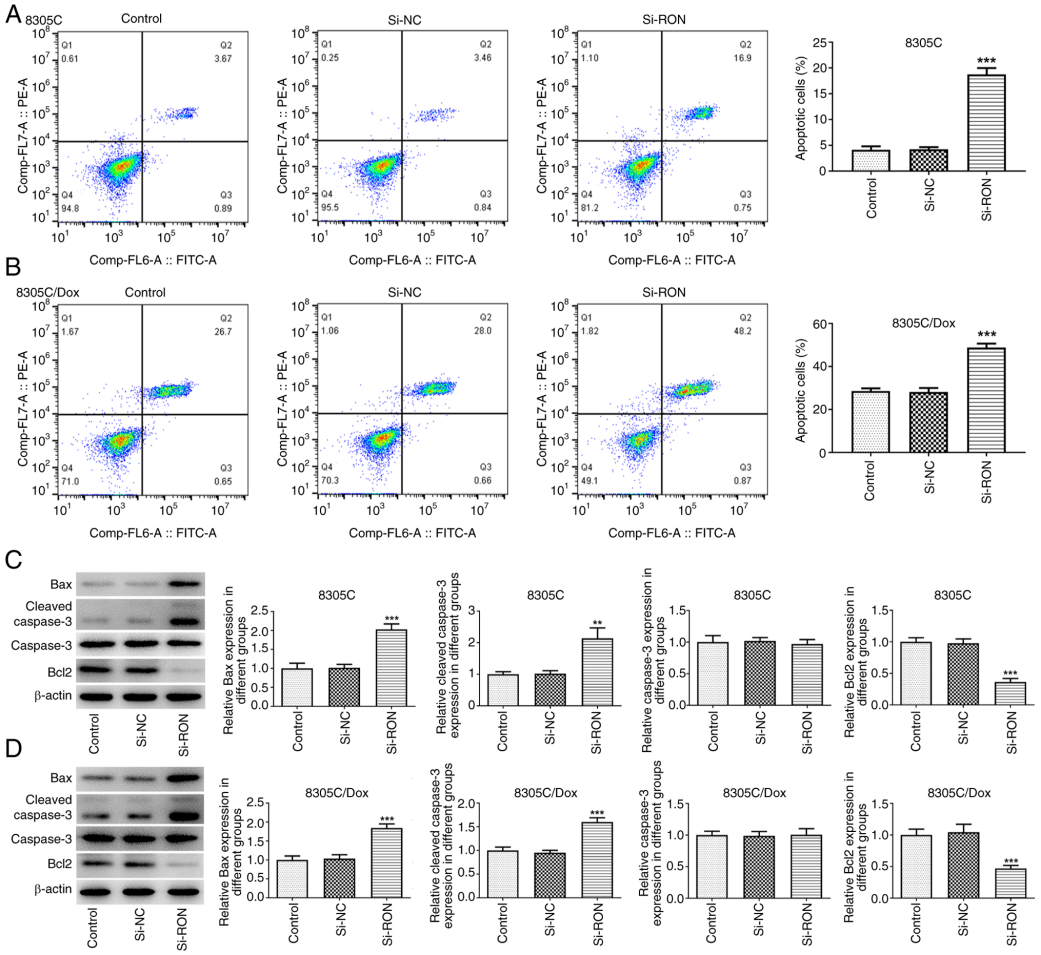

Figure 4. Effects of interference with RON on Dox resistance in thyroid cancer cells. (A) The apoptosis rate of 8305C cells were detected by flow cytometry; (B) apoptosis rate of 8305C/Dox cells were detected by flow cytometry; (C) expression of apoptosis-related proteins Bax, cleaved caspase3, caspase3 and Bcl2 in 8305C cells were estimated by western blotting; (D) expression of apoptosis-related proteins Bax, cleaved caspase3, caspase3 and Bcl2 in 8305C/Dox cells were estimated by western blotting. **P<0.01, ***P<0.001 vs. si-NC. NC, negative control; Dox, doxorubicin.

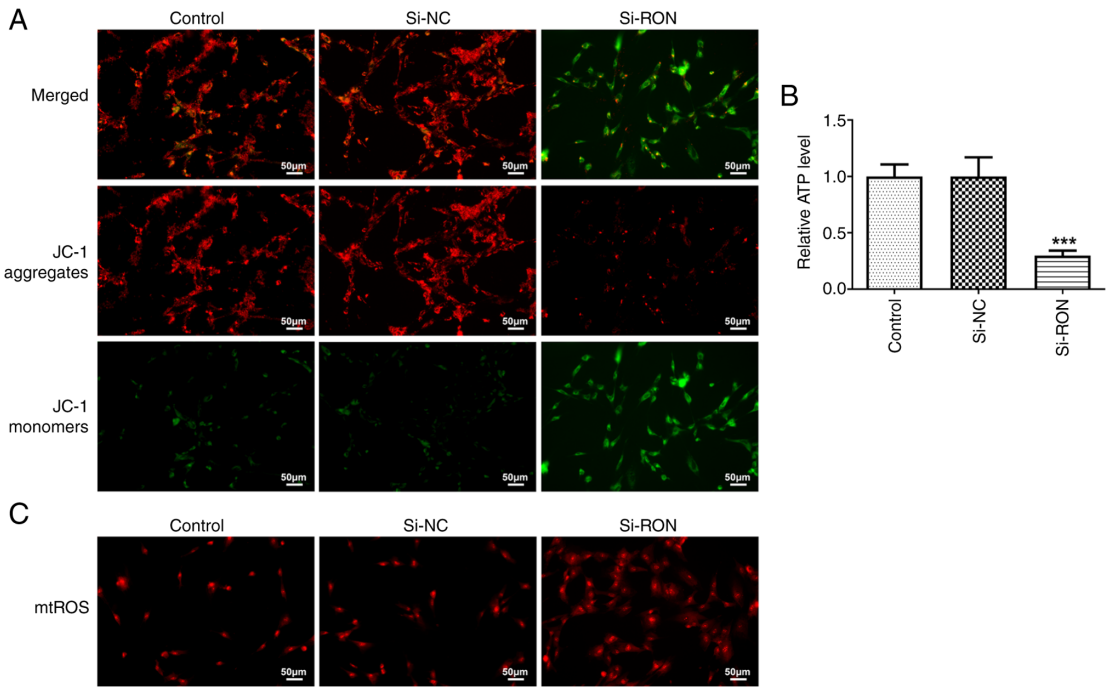

Figure 5. Effects of interference with RON on mitochondrial function in thyroid cancer cells. (A) Mitochondrial membrane potential was detected using a JC-1 fluorescence probe; (B) ATP content; (C) mtROS content. ***P<0.001 vs. si-NC. NC, negative control; JC-1, mtROS, mitochondrial reactive oxygen species.

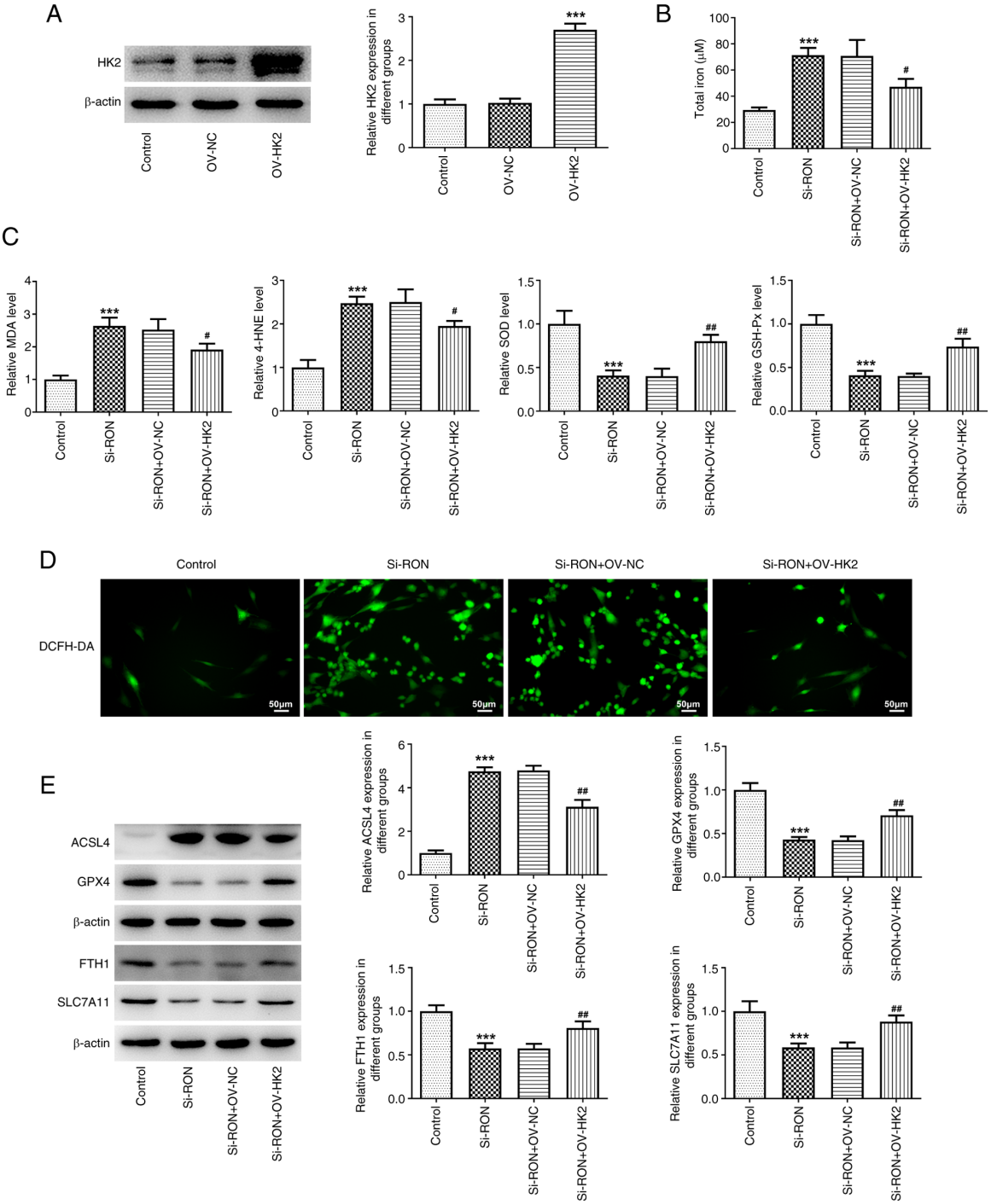

Figure 6. Effects of interference with RON on ferroptosis levels in thyroid cancer cells by inhibiting the glycolysis process. (A) Relative HK2 protein expression after overexpression. (B) total iron levels; (C) levels of MDA, 4-HNE, SOD and GSH-Px levels; (D) intracellular ROS levels; (E) protein levels of ferroptosis-related proteins ACSL4, GPX4, FTH1 and SLC7A11 were estimated by western blotting. ***P<0.001 vs. control, $^{\#}$P<0.05, $^{\#\#}$P<0.01 vs. si-RON+OV-NC. NC, negative control; MDA; malondialdehyde; 4-HNE, 4-hydroxynonenal; SOD, superoxide dismutase; GSH-Px, glutathione peroxidase; ACSL4, acyl-CoA synthetase long chain family member 4; GPX4, glutathione peroxidase 4; FTH1, ferritin heavy chain 1; SLC7A11, solute carrier family 7 member 11; HK2, hexokinase 2; DCFH-DA, 20,70-dichlorofluorescein diacetate.

mitochondrial function of thyroid cancer cells by regulating HK2 in glycolysis.

RON interference affects glycolysis by regulating MAPK/CREB signaling. To explore whether RON affects glycolysis by regulating MAPK/CREB signaling in thyroid cancer cells, western blotting was used to detect the expression levels of proteins related to the MAPK/CREB signaling pathway. The results demonstrated that the levels of phosphorylated (p-)p38 MAPK, p-CREB and p-Erk1/2 in thyroid cancer cells were markedly downregulated after RON interference (Fig. 9A and B). Subsequently, to further explore the effect of RON on glycolysis in thyroid cancer cells via MAPK/CREB signaling, the p38 MAPK agonist P79350 was added to 8305C cells. The results demonstrated that, compared with the si-RON group, the si-RON + P79350 group exhibited markedly increased

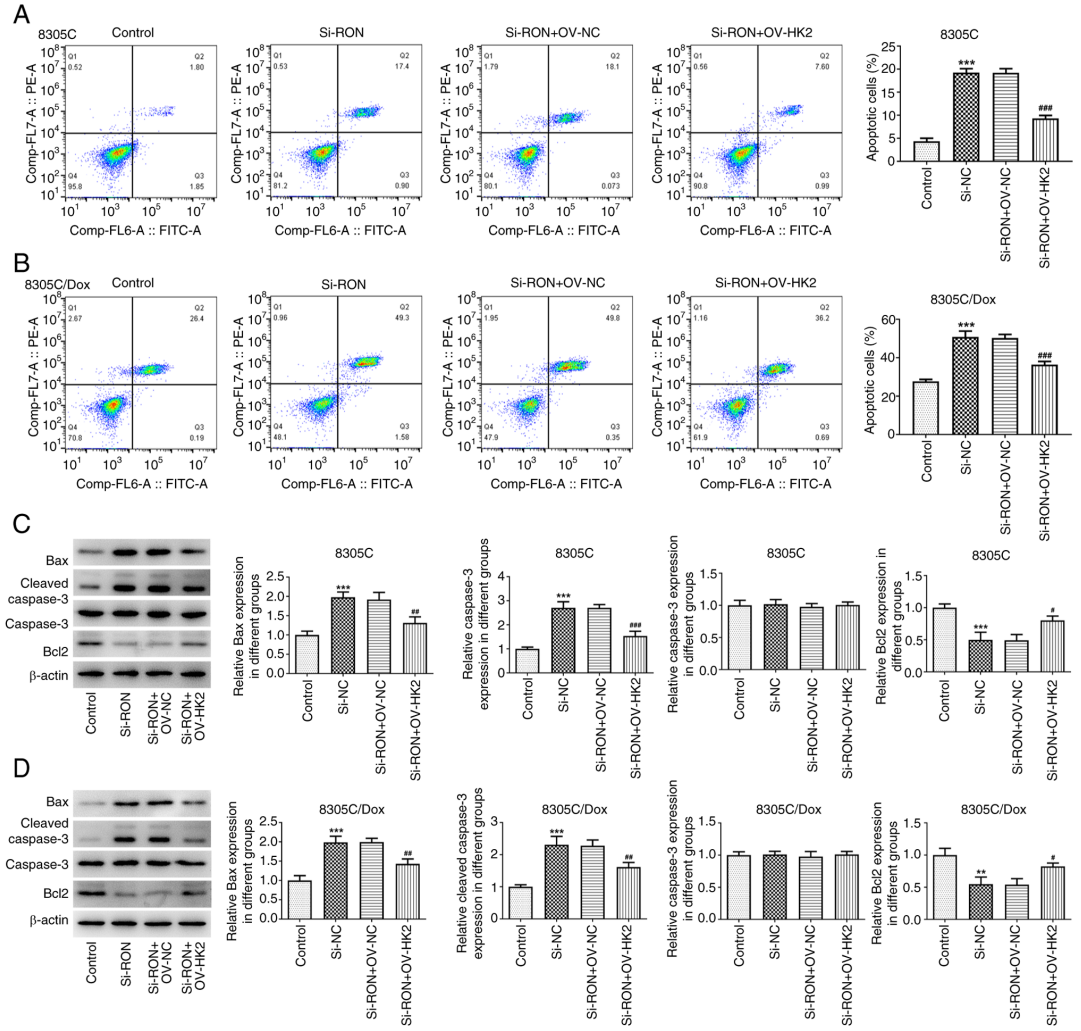

Figure 7. Effects of interference with RON on chemotherapy sensitivity of thyroid cancer cells by regulating HK2 in glycolysis. (A) Apoptosis rate of 8305C cells was detected by flow cytometry; (B) apoptosis rate of 8305C/Dox cells was detected by flow cytometry; (C) expression of apoptosis-related proteins Bax, cleaved caspase3, caspase3 and Bcl2 in 8305C cells were estimated by western blotting; (D) expression of apoptosis-related proteins Bax, cleaved caspase3, caspase3 and Bcl2 in 8305C/Dox cells were estimated by western blotting. **P<0.01, ***P<0.001 vs. control, $^{\#}$P<0.05, $^{\#\#}$P<0.01, $^{\#\#\#}$P<0.001 vs. si-RON+OV-NC. NC, negative control; Dox, doxorubicin.

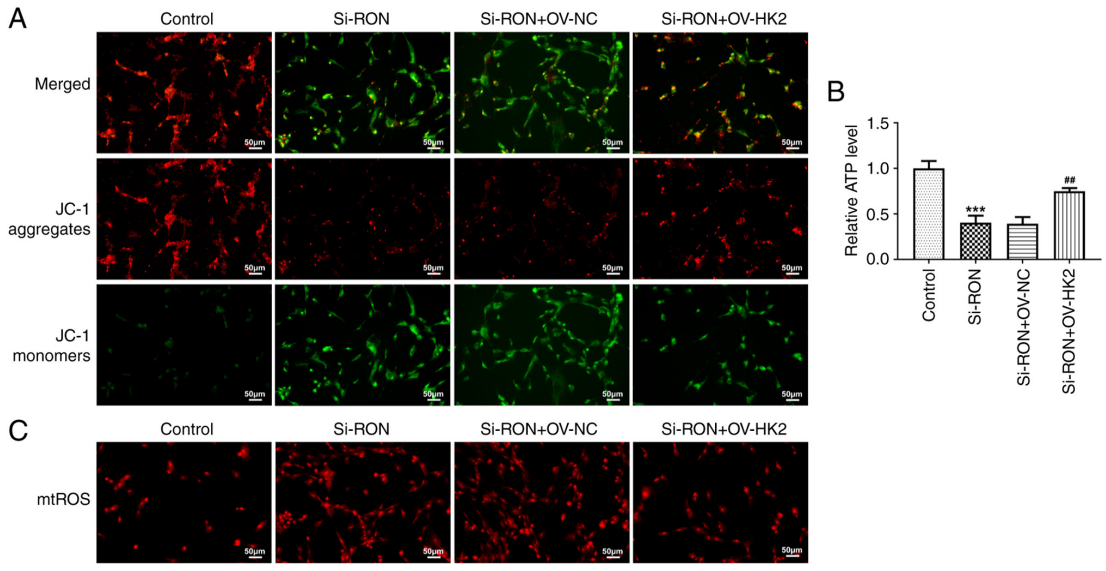

Figure 8. Effects of interference with RON on mitochondrial function in thyroid cancer cells by regulating HK2 in glycolysis. (A) Mitochondrial membrane potential was detected using a JC-1 fluorescence probe; (B) ATP content; (C) mtROS content. ***P<0.001 vs. control, $^{\#\#}$P<0.01 vs. si-RON+OV-NC. NC, negative control; JC-1, mtROS, mitochondrial reactive oxygen species; HK2, hexokinase 2.

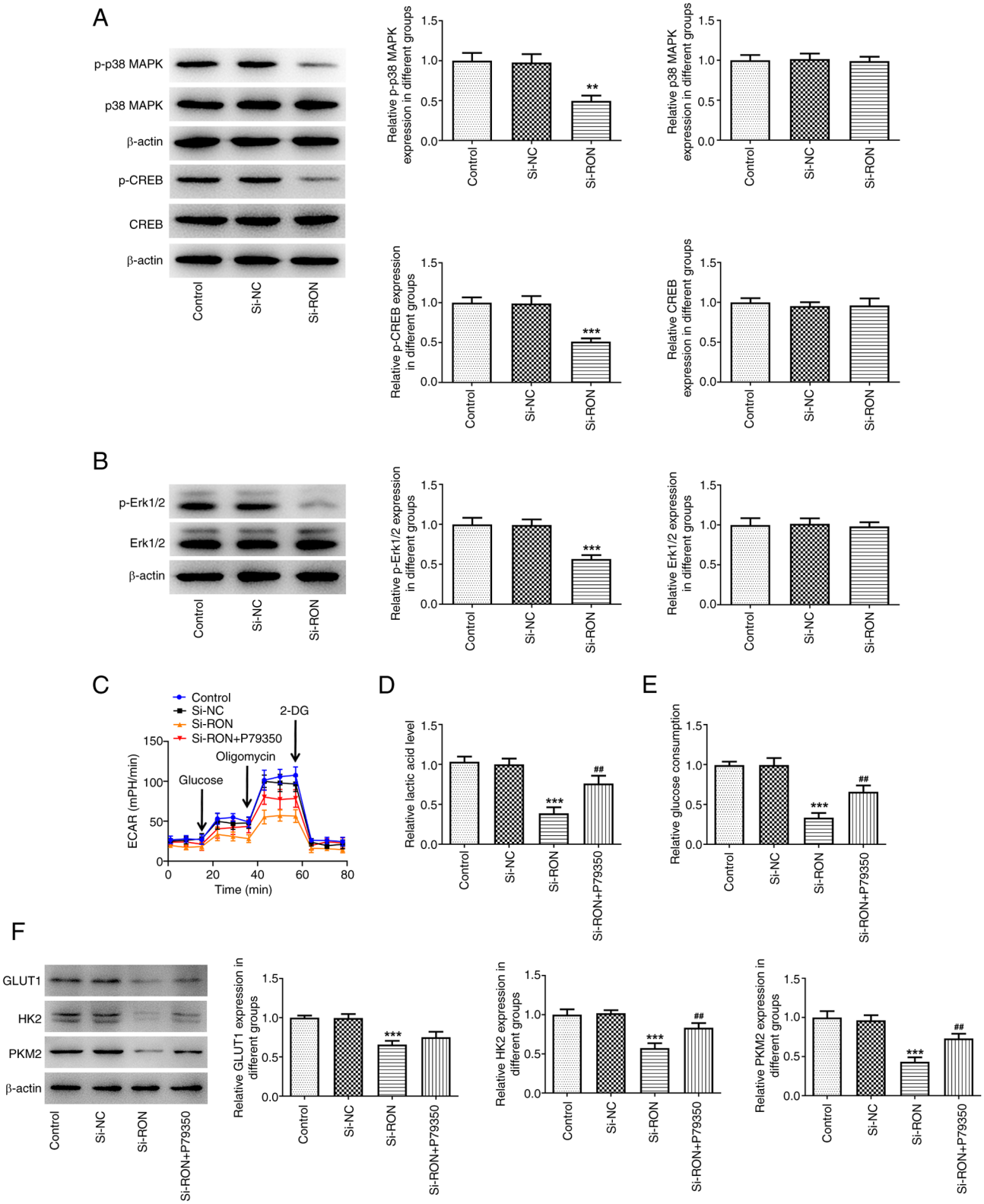

Figure 9. Effects of interference with RON on glycolysis through MAPK/CREB signaling. (A) Expression levels of proteins related to the MAPK/CREB signaling were assessed using western blotting; (B) expression levels of proteins p-Erk1/2 and Erk1/2 were assessed using western blotting, ***P<0.001 vs. si-NC; (C) ECAR assessment; (D) levels of lactic acid; (E) levels of glucose; (F) protein levels of GLUT1, HK2, PKM2 were estimated by western blotting. **P<0.01, ***P<0.001 vs. control, ##P<0.01, ###P<0.001 vs. si-RON. p-, phosphorylated; ECAR, extracellular acidification rate; HK2, hexokinase 2; GLUT1, glucose transporter 1; PKM2, pyruvate kinase M1/2; NC, negative control.

ECAR, lactate and glucose levels in the culture medium by affecting MAPK/CREB signaling in 8305C cells (Fig. 9C-E). Western blotting demonstrated that the expression levels of GLUT1, HK2 and PKM2 were increased in the si-RON + P79350 group (Fig. 9F). These results suggested that RON interference affected glycolysis via MAPK/CREB signaling.

Discussion

ATC is a rare, highly aggressive malignant tumor (25). There exists no effective or standard therapy for the treatment of ATC (26). Therefore, it is an urgent issue to explore the underlying molecular mechanisms involved in the initiation and progression of ATC as a greater number of novel candidate targets are needed to improve treatment decisions. The present data demonstrated that RON expression was markedly higher in thyroid cancer cell lines compared with the Nthy-ori 3-1 normal human thyroid cell line. Targeting RON may provide promising therapeutic approaches for the treatment of patients with ATC.

RON RTK is overexpressed in more than half of human breast cancers and can upregulate the glycolytic enzyme HK2 (16). The present results are similar to a previous study where RON interference inhibited glycolysis in thyroid cancer cells, and RON interference had the most obvious effect on HK2 in glycolysis (27). Previous research has revealed that ferroptosis serves a crucial role in ischemic organ damage, neurodegenerative diseases such as Alzheimer's disease and Parkinson's disease, and tumor cell death (28). Therefore, the present study explored the role of RON in the ferroptosis process in thyroid cancer. The present results demonstrated that RON interference increased ferroptosis levels in thyroid cancer cells.

Activation of RON RTK can confer resistance to tamoxifen in breast cancer cell lines, while silencing of RON receptor signaling can promote apoptosis and gemcitabine sensitivity in pancreatic cancer (29,30). Notably, in breast cancer, BMS-777607 (a RON tyrosine kinase inhibitor) can increase resistance to cytotoxic chemotherapy drugs, including Dox (31). However, the mechanism of RON on the chemotherapy drug Dox has not been fully characterized. The results of the present study revealed that RON interference increased the sensitivity of 8305C/Dox cells to apoptotic cell death, with a higher percentage of apoptotic cells, increased expression of Bax (pro-apoptotic) and cleaved caspase 3, which indicated that RON interference was associated with Dox resistance in 8305C cells. Furthermore, iron overload caused cardiac mitochondrial dysfunction, as indicated by increased mitochondrial ROS levels and mitochondrial membrane potential depolarization (32). Thus, the present study subsequently detected the mitochondrial function in thyroid cancer cells after RON interference, and the data indicated that RON interference affected mitochondrial function in thyroid cancer cells.

Previous result revealed that RON interference had the most notable effect on HK2 in glycolysis (16). A novel study also demonstrated that the key glycolysis gene HK2 could affect the ferroptosis process of tumor cells, and the most direct manifestation of ferroptosis was abnormal lipid metabolism (33). Therefore, the present study further explored whether the mechanism by which RON affects ferroptosis is related to the key glycolysis gene HK2. The present study demonstrated that RON interference affected the level of ferroptosis in thyroid cancer cells by inhibiting the HK2-mediated glycolytic process. In previous research, higher HK2 expression has been associated with chemoresistance in ovarian cancer (34). However, whether HK2 functionally contributes to chemotherapy sensitivity in ATC remains unclear. The present study explored the effect of RON interference on chemotherapy sensitivity of thyroid cancer cells by regulating HK2-mediated glycolysis. The results suggested that RON interference affected the chemotherapy sensitivity of thyroid cancer cells by regulating HK2-mediated glycolysis. A recent study delineated a crucial role of HK2 in governing glycolytic flux and mitochondrial activity, thereby modulating microglial functions in maladaptive inflammation in brain diseases (35). The present study also revealed that RON interference affected mitochondrial function in thyroid cancer cells by regulating HK2 in glycolysis.

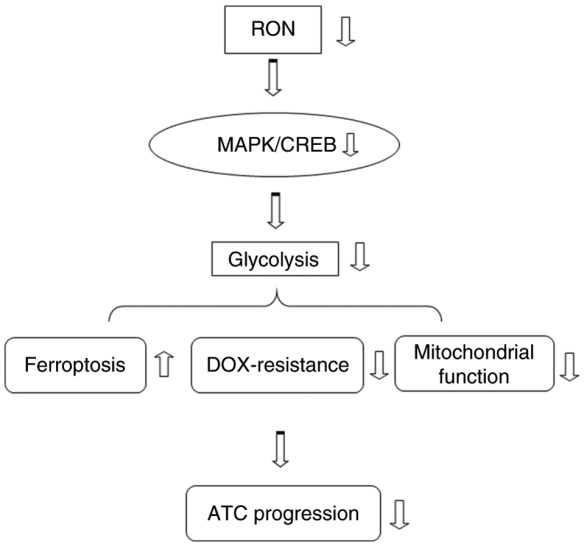

Figure 10. Summary of the present study. RON, recepteur d'origine nantais; MAPK, mitogen-activated protein kinase; CREB, cAMP-response element binding protein; Dox, doxorubicin; ATC, Anaplastic thyroid cancer.

A previous study demonstrated that RON activated the MAPK/RSK/CREB signaling pathway to enhance C-X-C motif chemokine receptor 4 expression and promote cell migration and invasion in bladder cancer (18). Furthermore, CREB, which is associated with proliferation in thyroid cancer, serves a role in the proliferation of normal thyroid follicular cells (36,37). Furthermore, activating mutations in the MAPK pathway serve an important role in ATC (38). However, there are few studies on whether RON could regulate glycolysis through MAPK/CREB signaling. Therefore, the present study evaluated the expression levels of proteins related to the MAPK/CREB signaling pathway. The results indicated that RON interference reduced the levels of p-p38 MAPK, p-CREB and p-Erk1/2 in thyroid cancer cells, and increased ECAR, lactate and glucose levels in the culture medium by affecting MAPK/CREB signaling. These findings demonstrated that RON interference affected glycolysis via MAPK/CREB signaling. Based on the results of the present study, future endeavors will investigate whether RON can regulate the ATC process through other mechanisms affecting glycolysis and ferroptosis, and the mechanisms with which RON can be administered for patients with ATC. Furthermore, the present study did not involve animal and clinical studies, which should be performed in future experiments to confirm the findings of the present study.

In conclusion, the present observations revealed that RON silencing modulated glycolysis via the MAPK/CREB signaling pathway, thereby promoting ferroptosis and chemotherapy sensitivity of thyroid cancer cells (Fig. 10). RON may serve as a potential therapeutic opportunity for ATC treatment.

Acknowledgements

Not applicable.

Funding

The present study received funding from the Zhejiang Public Welfare Technology Applied Research Project (grant no. LGF18H160014) and College Student's Science and Technology Innovation Activity Plan of Zhejiang Province (grant no. 2023R465020).

Availability of data and materials

The data generated in the present study may be requested from the corresponding author.

Authors' contributions

XJ conceived and designed the study, and contributed to the writing of the manuscript; HZ and XC acquired and interpreted the data; and YY and DS collected and analyzed the data. XJ and HZ confirm the authenticity of all the raw data. All authors read and approved the final version of the manuscript.

Ethics approval and consent to participate

Not applicable.

Patient consent for publication

Not applicable.

Competing interests

The authors declare that they have no competing interests.

References

1. Sung H, Ferlay J, Siegel RL, Laversanne M, Soerjomataram I, Jemal A and Bray F: Global cancer statistics 2020: GLOBOCAN estimates of incidence and mortality worldwide for 36 cancers in 185 countries. CA Cancer J Clin 71: 209-249, 2021.
2. Ragazzi M, Ciarrocchi A, Sancisi V, Gandolfi G, Bisagni A and Piana S: Update on anaplastic thyroid carcinoma: Morphological, molecular, and genetic features of the most aggressive thyroid cancer. Int J Endocrinol 2014: 790834, 2014.
3. Nagaiah G, Hossain A, Mooney CJ, Parmentier J and Remick SC: Anaplastic thyroid cancer: A review of epidemiology, pathogenesis and treatment. J Oncol 2011: 542358, 2011.
4. Smallridge RC, Ain KB, Asa SL, Bible KC, Brierley JD, Burman KD, Kebebew E, Lee NY, Nikiforov YE, Rosenthal MS, *et al*: American thyroid association guidelines for management of patients with anaplastic thyroid cancer. Thyroid 22: 1104-1139, 2012.
5. Molinaro E, Romei C, Biagini A, Sabini E, Agate L, Mazzeo S, Materazzi G, Sellari-Franceschini S, Ribechini A, Torregrossa L, *et al*: Anaplastic thyroid carcinoma: From clinicopathology to genetics and advanced therapies. Nat Rev Endocrinol 13: 644-660, 2017.
6. Kebebew E, Greenspan FS, Clark OH, Woeber KA and McMillan A: Anaplastic thyroid carcinoma. Treatment outcome and prognostic factors. Cancer 103: 1330-1335, 2005.
7. Are C and Shaha AR: Anaplastic thyroid carcinoma: Biology, pathogenesis, prognostic factors, and treatment approaches. Ann Surg Oncol 13: 453-464, 2006.
8. Sasanakietkul T, Murtha TD, Javid M, Korah R and Carling T: Epigenetic modifications in poorly differentiated and anaplastic thyroid cancer. Mol Cell Endocrinol 469: 23-37, 2018.
9. Saini S, Maker AV, Burman KD and Prabhakar BS: Molecular aberrations and signaling cascades implicated in the pathogenesis of anaplastic thyroid cancer. Biochim Biophys Acta Rev Cancer 1872: 188262, 2019.
10. Robertson SC, Tynan J and Donoghue DJ: RTK mutations and human syndromes: When good receptors turn bad. Trends Genet 16: 368, 2000.
11. Adams GP and Weiner LM: Monoclonal antibody therapy of cancer. Nat Biotechnol 23: 1147-1157, 2005.
12. Geng L, Wang XT, Yu J and Yang YL: Antagonism of cortistatin against cyclosporine-induced apoptosis in rat myocardial cells and its effect on myocardial apoptosis gene expression. Eur Rev Med Pharmacol Sci 22: 3207-3213, 2018.
13. Ronsin C, Muscatelli F, Mattei MG and Breathnach R: A novel putative receptor protein tyrosine kinase of the met family. Oncogene 8: 1195-1202, 1993.
14. Camp ER, Liu W, Fan F, Yang A, Somcio R and Ellis LM: RON, a tyrosine kinase receptor involved in tumor progression and metastasis. Ann Surg Oncol 12: 273-281, 2005.
15. Wang MH, Lee W, Luo YL, Weis MT and Yao HP: Altered expression of the RON receptor tyrosine kinase in various epithelial cancers and its contribution to tumourigenic phenotypes in thyroid cancer cells. J Pathol 213: 402-411, 2007.
16. Hunt BG, Davis JC, Fox LH, Vicente-Muñoz S, Lester C, Wells SI and Waltz SE: RON-augmented cholesterol biosynthesis in breast cancer metastatic progression and recurrence. Oncogene 42: 1716-1727, 2023.
17. Zheng XJ, Chen WL, Yi J, Li W, Liu JY, Fu WQ, Ren LW, Li S, Ge BB, Yang YH, *et al*: Apolipoprotein C1 promotes glioblastoma tumorigenesis by reducing KEAP1/NRF2 and CBS-regulated ferroptosis. Acta Pharmacol Sin 43: 2977-2992, 2022.
18. Chen J, Wang K, Ye S, Meng X, Jia X, Huang Y and Ma Q: Tyrosine kinase receptor RON activates MAPK/RSK/CREB signal pathway to enhance CXCR4 expression and promote cell migration and invasion in bladder cancer. Aging (Albany NY) 14: 7093-7108, 2022.
19. Ma X, Xu J, Gao N, Tian J and Song T: Dexmedetomidine attenuates myocardial ischemia-reperfusion injury via inhibiting ferroptosis by the cAMP/PKA/CREB pathway. Mol Cell Probes 68: 101899, 2023.
20. Sun RF, Zhao CY, Chen S, Yu W, Zhou MM and Gao CR: Androgen receptor stimulates hexokinase 2 and induces glycolysis by PKA/CREB signaling in hepatocellular carcinoma. Dig Dis Sci 66: 802-813, 2021.
21. Farhat D, Ghayad SE, Icard P, Le Romancer M, Hussein N and Lincet H: Lipoic acid-induced oxidative stress abrogates IGF-1R maturation by inhibiting the CREB/furin axis in breast cancer cell lines. Oncogene 39: 3604-3610, 2020.
22. Xu Y, Han YF, Ye B, Zhang YL, Dong JD, Zhu SJ and Chen J: miR-27b-3p is involved in doxorubicin resistance of human anaplastic thyroid cancer cells via targeting peroxisome proliferator-activated receptor gamma. Basic Clin Pharmacol Toxicol 123: 670-677, 2018.
23. Sakamuru S, Zhao J, Attene-Ramos MS and Xia M: Mitochondrial membrane potential assay. Methods Mol Biol 2474: 11-19, 2022.
24. Park JS, Choi HI, Kim DH, Kim CS, Bae EH, Ma SK and Kim SW: RON receptor tyrosine kinase regulates epithelial mesenchymal transition and the expression of pro-fibrotic markers via Src/Smad signaling in HK-2 and NRK49F cells. Int J Mol Sci 20: 5489, 2019.
25. Bible KC, Kebebew E, Brierley J, Brito JP, Cabanillas ME, Clark TJ Jr, Di Cristofano A, Foote R, Giordano T, Kasperbauer J, *et al*: 2021 American thyroid association guidelines for management of patients with anaplastic thyroid cancer. Thyroid 31: 337-386, 2021.
26. Tang J, Yang Q, Mao C, Xiao D, Liu S, Xiao L, Zhou L, Wu G and Tao Y: The deubiquitinating enzyme UCHL3 promotes anaplastic thyroid cancer progression and metastasis through hippo signaling pathway. Cell Death Differ 30: 1247-1259, 2023.
27. Davis JC and Waltz SE: The MET family of receptor tyrosine kinases promotes a shift to pro-tumor metabolism. Genes 15: 953, 2024.
28. Qiu Y, Cao Y, Cao W, Jia Y and Lu N: The application of ferroptosis in diseases. Pharmacol Res 159: 104919, 2020.

29. McClaine RJ, Marshall AM, Wagh PK and Waltz SE: Ron receptor tyrosine kinase activation confers resistance to tamoxifen in breast cancer cell lines. Neoplasia 12: 650-658, 2010.
30. Logan-Collins J, Thomas RM, Yu P, Jaquish D, Mose E, French R, Stuart W, McClaine R, Aronow B, Hoffman RM, *et al*: Silencing of RON receptor signaling promotes apoptosis and gemcitabine sensitivity in pancreatic cancers. Cancer Res 70: 1130-1140, 2010.
31. Sharma S, Zeng JY, Zhuang CM, Zhou YQ, Yao HP, Hu X, Zhang R and Wang MH: Small-molecule inhibitor BMS-777607 induces breast cancer cell polyploidy with increased resistance to cytotoxic chemotherapy agents. Mol Cancer Ther 12: 725-736, 2013.
32. Kumfu S, Chattipakorn S, Fucharoen S and Chattipakorn N: Mitochondrial calcium uniporter blocker prevents cardiac mitochondrial dysfunction induced by iron overload in thalassemic mice. Biometals 25: 1167-1175, 2012.
33. Dai YQ, Bai Y, Gu J and Fan BY: Stanniocalcin1 knockdown induces ferroptosis and suppresses glycolysis in prostate cancer via the Nrf2 pathway. Neoplasma 69: 1396-1405, 2022.
34. Zhang XY, Zhang M, Cong Q, Zhang MX, Zhang MY, Lu YY and Xu CJ: Hexokinase 2 confers resistance to cisplatin in ovarian cancer cells by enhancing cisplatin-induced autophagy. Int J Biochem Cell Biol 95: 9-16, 2018.
35. Fang J, Luo S and Lu Z: HK2: Gatekeeping microglial activity by tuning glucose metabolism and mitochondrial functions. Mol Cell 83: 829-831, 2023.
36. Siu YT and Jin DY: CREB-a real culprit in oncogenesis. FEBS J 274: 3224-3232, 2007.
37. Nguyen LQ, Kopp P, Martinson F, Stanfield K, Roth SI and Jameson JL: A dominant negative CREB (cAMP response element-binding protein) isoform inhibits thyrocyte growth, thyroid-specific gene expression, differentiation, and function. Mol Endocrinol 14: 1448-1461, 2000.
38. Scheffel RS, Dora JM and Maia AL: BRAF mutations in thyroid cancer. Curr Opin Oncol 34: 9-18, 2022.

Copyright © 2024 Jin et al. This work is licensed under a Creative Commons Attribution-NonCommercial-NoDerivatives 4.0 International (CC BY-NC-ND 4.0) License.